

## High Extinction Coefficient “Antenna” Dye in Solid-State Dye-Sensitized Solar Cells: A Photophysical and Electronic Study

Henry J. Snaith,<sup>\*,†</sup> C. S. Karthikeyan,<sup>‡</sup> Annamaria Petrozza,<sup>§</sup> Joël Teuscher,<sup>||</sup> Jacques E. Moser,<sup>||</sup> Mohammad K. Nazeeruddin,<sup>||</sup> Mukundan Thelakkat,<sup>‡</sup> and Michael Grätzel<sup>||</sup>

Clarendon Laboratory, Department of Physics, University of Oxford, Parks Road, Oxford, OX1 3PU United Kingdom, Applied Functional Polymers and Lab for Solar Energy Research, University of Bayreuth, 95440 Bayreuth, Germany, Cavendish Laboratory, University of Cambridge, J.J. Thomson Avenue, Cambridge, CB3 0HE United Kingdom, and Institut des Sciences et Ingénierie Chimiques, École Polytechnique Fédérale de Lausanne, CH-1015 Lausanne, Switzerland

Received: February 27, 2008; Revised Manuscript Received: April 8, 2008

We present a photophysical and device-based investigation of a new bipyridyl–NCS ruthenium complex sensitizer with an extended  $\pi$  system, in both sensitized TiO<sub>2</sub> and incorporated into solid-state dye-sensitized solar cells. We compare this new sensitizer to an analog dye without the extended  $\pi$  system. We observe very similar excited-state absorption spectra and charge recombination kinetics for the two systems. However, the  $\pi$ -extended sensitizer has a phenomenally enhanced molar extinction coefficient which translates into far greater light harvesting and current collection in solid-state dye-sensitized solar cells. We also infer from transient photovoltage measurements that positioning the pendent extended  $\pi$  system away from the TiO<sub>2</sub> surface has induced a favorable dipole shift, generating enhanced open-circuit voltage. The resulting power conversion efficiency for the solar cell has been increased from 2.4% to 3.2% when comparing the new sensitizer to an analogy with no pendent group.

### Introduction

Photosynthesis in plants occurs following light absorption in dye chromophores with subsequent charge generation and separation via a cascade in energy through a sequence of molecules in order to spatially separate the photogenerated electron and hole. A “synthetic” photovoltaic system close to natural photosynthesis is the dye-sensitized solar cell. Here, light is absorbed in a molecular sensitizer, which is chemisorbed to a mesostructured TiO<sub>2</sub> electrode, with subsequent electron transfer to the TiO<sub>2</sub>. For the solid-state dye-sensitized solar cells studied herein, the dye molecules are contacted on the other side by an organic hole transporting material 2,2',7,7'-tetrakis(*N,N*-dimethoxyphenyl-amine)-9,9'-spirobifluorene (Spiro-MeOTAD) to which hole transfer takes place, regenerating the oxidized dye. The insertion of a further charge transfer step between the dye and the Spiro-MeOTAD has been postulated to increase the average spatial separation of the electrons and holes and thus reduce recombination losses and increase device efficiency. There have been recent spectroscopic studies investigating the recombination kinetics of “donor-acceptor” dyes adsorbed to TiO<sub>2</sub> surfaces.<sup>1–3</sup> Donor-acceptor dyes have an electron donating unit attached directly to the dye core and have been shown to facilitate hole transfer from the dye chromophore to the appended unit.<sup>1</sup> For TiO<sub>2</sub> sensitized with these dyes, the

recombination rate constant between the electron injected into the TiO<sub>2</sub> and the hole on the dye molecule can be strikingly reduced by many orders of magnitude. This appears to be due to extending the average spatial separation of the electrons and holes.<sup>2,3</sup> However, as of yet these dyes have not performed favorably in complete solar cells, though some studies have demonstrated their potential utility.<sup>3</sup> A new series of “donor-acceptor” dyes have recently been developed which consist of a ruthenium complex with both NCS and bipyridyl ligands. This core corresponds to the standard ruthenium complex which has previously shown great performance in both solid-state and liquid electrolyte dye-sensitized solar cells.<sup>4,5</sup> To the periphery of one of the bipyridyl ligands, triphenyl amine (TPA) or *N,N'*-bis(phenyl)-*N,N'*-bis(3-methylphenyl)-1,10-biphenyl-4,4'-diamine (TPD) units are covalently linked. These dyes operate efficiently in DSCs and the reason for the efficient operation may be that they do facilitate a charge generation cascade and that the bulkiness of the appended electron-donor units increases the electron-hole separation and retards charge recombination. Spectroscopic studies of a series of these dyes incorporated in solid-state DSCs are indeed consistent with this postulation.<sup>6</sup> Here, we perform a spectroscopic and device based study on efficiently operating solid-state dye-sensitized solar cells, comparing a new TPA substituted dye to a standard NCS-bipyridyl-Ru complex with an identical core but a methyl unit in place of the appended TPA “electron-donating” unit. The pendent group conjugated to the dye core causes more than a doubling of the optical density in the ensuing films and a slightly red-shifted absorption spectrum. However, our spectroscopic studies reveal almost identical kinetics for the two dye systems, for

\* To whom correspondence should be addressed. E-mail: h.snaith1@physics.ox.ac.uk.

<sup>†</sup> University of Oxford.

<sup>‡</sup> University of Bayreuth.

<sup>§</sup> University of Cambridge.

<sup>||</sup> École Polytechnique Fédérale de Lausanne.

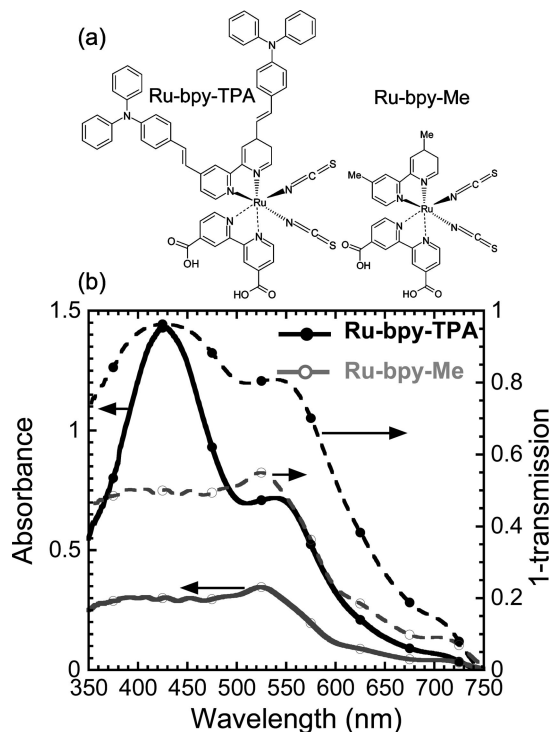


**Figure 1.** (a) Chemical structure of the two dye molecules used in this study. (b) UV-vis absorption spectra (solid lines) and 1-transmission spectra (dashed lines), for 1.4  $\mu\text{m}$  thick mesoporous  $\text{TiO}_2$  films coated on glass slides sensitized with Ru-bpy-TPA (dark lines, solid symbols) and Ru-bpy-Me (light gray lines, open symbols).

both the electron recombination reaction with the oxidized dye molecules and the recombination reaction with the holes in the Spiro-MeOTAD hole-transporter. In spite of this, the phenomenally enhanced molar extinction coefficient of the new dye results in augmented light absorption and significantly increased current collection efficiency and subsequent power conversion efficiency when incorporated in complete solar cells.

### Experimental Section

The new dye is comprised of a standard bipyridyl NCS ruthenium complex chromophore with a triphenylamine (TPA) pendant side group conjugated to the 4 and 4' positions of one of the nonchelating bipyridyl ligands, here, we will term it Ru-bpy-TPA. The synthesis procedures are described elsewhere.<sup>7</sup> The  $\text{TiO}_2$  film preparation and dyeing procedures were identical to those previously described, along with the solar cell fabrication and characterization procedures.<sup>8</sup> Photoinduced absorption spectroscopy was performed using the procedure by Ford et al.,<sup>9</sup> and transient absorption spectroscopy was performed using the procedure by Moser et al.<sup>10</sup> The transient open-circuit voltage decay measurements were performed as previously described.<sup>11</sup>

### Results and Discussion

**Light Absorption.** We compare the Ru-bpy-TPA to a dye with an identical core structure, however, the TPA unit is replaced with a simple methyl unit, which we shall term Ru-bpy-Me. The chemical structures are shown in Figure 1 along with the absorption spectra of a 1.4  $\mu\text{m}$  thick film of mesoporous  $\text{TiO}_2$  sensitized with the dye molecules. The most striking feature in the absorption is the extreme enhancement at around 430 nm. The absorption peak for isolated TPA is around 300 nm. We do observe this peak in the absorption spectra of the dye solution demonstrating that the enhancement at 430 nm is

not purely due to absorption from the TPA unit but enhanced oscillator strength of the ruthenium "super-complex". Along with the overall enhanced absorption, there is a red-shift of the peak centered at 525 nm for the standard dye to 540 nm for the Ru-bpy-TPA, consistent with this dye having an extended  $\pi$ -conjugated system when compared to the methyl substituted molecule. The reduction in the optical bandgap corresponds to approximately 65 meV. In solution the molar extinction coefficient of Ru-bpy-Me is approximately  $13\,500\ \text{M}^{-1}\text{cm}^{-1}$  at 525 nm as compared to approximately  $20\,000\ \text{M}^{-1}\text{cm}^{-1}$  for Ru-bpy-TPA at 540 nm. The solution UV-vis absorption spectra are shown in the Supporting Information. This demonstrates that the enhanced absorption in the sensitized films is not an artifact of increased dye loading but predominantly due to the increased molar extinction coefficient of the complex.

**Photoinduced Absorption.** The relatively small red-shift in absorption suggests that a new charge transfer state between the original chromophore and the appended TPA unit has not been created, though it is consistent with some extent of delocalization of the  $\pi$  system on to the TPA unit. When the ruthenium complex sensitizer is adsorbed on to a  $\text{TiO}_2$  surface, electrons are considered to be injected very rapidly into the  $\text{TiO}_2$  upon light absorption in the dye (fs time scale). A hole is then left on the dye molecule which will eventually recombine with electrons in the  $\text{TiO}_2$  if the dye is not contacted to a regenerative medium such as Spiro-MeOTAD or iodide/triiodide redox couple. For the TPA substituted dye studied here, we investigate whether the hole undergoes a sequential transfer from the central chromophore to the TPA units. We have first performed photoinduced absorption (PIA) spectroscopy on 1.4  $\mu\text{m}$  thick mesoporous  $\text{TiO}_2$  films sensitized with the two dyes. Looking at the signal for the Ru-bpy-Me film we observe a bleaching of the signal above 2 eV ( $\sim 615$  nm) and a double peaked broad photoinduced absorption with one peak centered around 1.55 eV ( $\sim 800$  nm) and the higher energy feature overlapping with the bleaching signal, with the peak appearing at around 1.9 eV ( $\sim 650$  nm). These features are consistent with the absorption of the oxidized Ru-bpy-NCS complex previously observed.<sup>1</sup> The bleaching of the Ru-bpy-TPA signal is slightly red-shifted in comparison, consistent with the red-shifted absorption spectra. However, the main polaron absorption feature remains very similar to the Ru-bpy-Me sample. There are subtle differences between these spectrums however, which we will explain and interpret here: For the Ru-bpy-TPA, the PIA signal at 1.55 eV is approximately the same intensity as for the Ru-bpy-Me, even though the absorption of the excitation light is much greater. In the far-infrared region (1.1–1.2 eV), where the electron absorbs in the  $\text{TiO}_2$ , the signal for the Ru-bpy-TPA is much stronger than for the Ru-bpy-Me, consistent with a larger photogenerated electron density. In contrast to the Ru-bpy-Me bleaching signal in the visible, for the Ru-bpy-TPA the photobleaching is dominated by a new photoinduced absorption, resulting in an overall negative signal from 2.4 eV onward. We interpret this as there indeed being more charge generated from the Ru-bpy-TPA, apparent from the increased light absorption by electron species in the  $\text{TiO}_2$ . If the polaron on the TPA unit absorbs in the visible region of the spectrum, then the change to the visible and near IR region of the spectrum can be interpreted as the polaron being delocalized over the entire  $\pi$  system, with significant HOMO density residing on the TPA unit. In fact this is a very similar effect to that observed when a hole-transporter, such as Spiro-MeOTAD, is in contact with a standard ruthenium complex.<sup>12</sup> The interesting question here is whether a delocalized polaron with a broad absorption

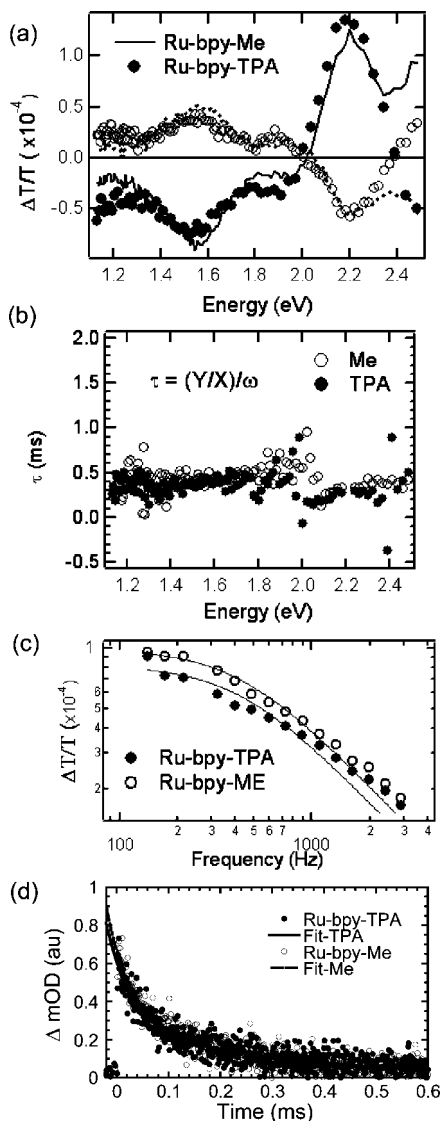


**Figure 2.** (a) Photo induced absorption (PIA) spectra for 1.4  $\mu\text{m}$  thick mesoporous  $\text{TiO}_2$  films sensitized with Ru-bpy-TPA (circles) and Ru-bpy-Me (lines), pumped at 488 nm with an intensity of 128  $\text{mWcm}^{-2}$  and a frequency of 200 Hz under dynamic vacuum. The open circles and the dashed line correspond to the out-of-phase signals for the Ru-bpy-TPA and Ru-bpy-Me, respectively. And the solid circles and solid line correspond to the in phase signal. Please note that the lines without symbols are real data for the Ru-bpy-Me sensitized films and not guides to the eye. (b) The estimated “lifetime” of the photoinduced absorption signal, calculated from the data presented in (a), as a function of photon energy for the Ru-bpy-Me (open circles) and Ru-bpy-TPA (solid circles) sensitized samples. (c) The frequency dependence of the PIA signal ( $dr = (dx^2 + dy^2)^{1/2}$  at 800 nm (1.55 eV) under the same pump beam conditions as above. d) Transient absorption spectroscopy (TAS) of two similar samples to above, Ru-bpy-TPA (dark solid circles, solid line) and Ru-bpy-ME (gray open circles, dashed line) of the transient absorption signal at 650 nm ( $\sim 1.9$  eV absorption of the oxidized dye species). The pump was at 600 nm with a pulse width of  $\sim 5$  ns with 35  $\mu\text{J/pulse}$  and a repetition rate of 30 Hz.

exists or if there is sequential hole transfer from the basic ruthenium complex core to the TPA unit. In order to estimate the lifetime of each species, we can compare the magnitude of the in phase (X) and out of phase (Y) spectrum following the procedure of Westerling et al. where the lifetime ( $\tau$ ) is given by  $\tau = (Y/X)/\omega$ , where  $\omega$  is the modulation frequency.<sup>13</sup> This is presented in Figure 2b for both Ru-bpy-TPA and Ru-bpy-Me spectra. The data is reasonably noisy, especially where the PIA signal is small; however, it is quite clear that there is

not a significant variation in the estimated lifetime between the species or between the dye molecules. The lifetime is approximately 400  $\mu\text{s}$ . This is reasonably strong evidence that a delocalized polaron exists and that a sequential charge transfer does not take place in this system.

In order to probe the lifetime more accurately, the species lifetime can be estimated by scanning the PIA signal over a broad range of modulation frequencies. Figure 2c shows the frequency dependence of the PIA signal measured at 800 nm, with 128  $\text{mWcm}^{-2}$  illumination intensity. The ideal behavior expected for species with a well defined lifetime should show the PIA signal independent of modulation frequency ( $\omega$ ) at lower modulation frequencies and a decrease as a power law of  $\omega^{-1}$  at higher frequencies according to:

$$\frac{\Delta T}{T} = \frac{N\tau}{\sqrt{(\omega\tau)^2 + 1}} \quad (1)$$

Here, this simple model is not completely accurate at higher frequency for both samples, whose signal decreases with a power law  $\omega^{-a}$  with  $a < 1$ , characteristic of a distribution of lifetimes for the electrons in the  $\text{TiO}_2$ . Though it is not an ideal situation, it is still possible to fit the data with eq 1 in order to obtain an approximate, or average, lifetime for the charge species. We find very similar lifetimes for the two dyes with  $370 \pm 30 \mu\text{s}$  for Ru-bpy-Me and  $380 \pm 40 \mu\text{s}$  for Ru-bpy-TPA. This is also in very good agreement with the previous estimation above.

**Transient Absorption Spectroscopy.** In order to confirm the PIA measurements with a separate technique, we have also performed microsecond to millisecond transient absorption spectroscopy on mesoporous  $\text{TiO}_2$  films sensitized with the two dyes. Figure 2d shows the transient absorption signal for the two systems, pumping at 600 nm and measuring the change in absorption of the oxidized dye species at 650 nm (the pump intensity was 35  $\mu\text{J/pulse}$ ). We observe moderately fast recombination of the electrons with the oxidized Ru-bpy-Me, exhibiting a reaction half-time,  $t_{50\%}$ , of approximately 60  $\mu\text{s}$ . Consistent with the PIA measurements, we observe almost identical kinetics for the two dyes, with the reaction for the film containing Ru-bpy-TPA also exhibiting a half-time of approximately 60  $\mu\text{s}$ . There is a difference in the kinetic data reported previously<sup>6</sup> and those reported here, which may be due to the difference in the experimental conditions such as intensity of light used, degree of dye absorption, etc. To compare the results here with a standard ruthenium complex, we observe a recombination half-time of approximately 200  $\mu\text{s}$  for “Z907” measured under the same conditions.<sup>14</sup> Z907 is a standard ruthenium complex which operates very efficiently in this solid-state photovoltaic system.<sup>15</sup> If this recombination reaction is governed by the tunneling distance between the electrons and holes then these measurements suggests that the distance between the electrons in the  $\text{TiO}_2$  and the highest occupied molecular orbitals (HOMOs) on the dye molecules are very similar for the systems studied here, consistent with a large fraction of the HOMOs still residing on the NCS ligands.

**Dye-Sensitized Solar Cell Performance.** We have fabricated complete solid-state dye-sensitized solar cells in order to verify that the enhanced absorption translates into increased current-collection. In Figure 3a, we present the photovoltaic action spectra for devices fabricated with Ru-bpy-TPA and Ru-bpy-Me. We do indeed observe significantly enhanced current collection with an approximate doubling of the incident-photon to collected-electron quantum efficiency (IPCE) at most wavelengths. By considering the absorption spectrum (presented as



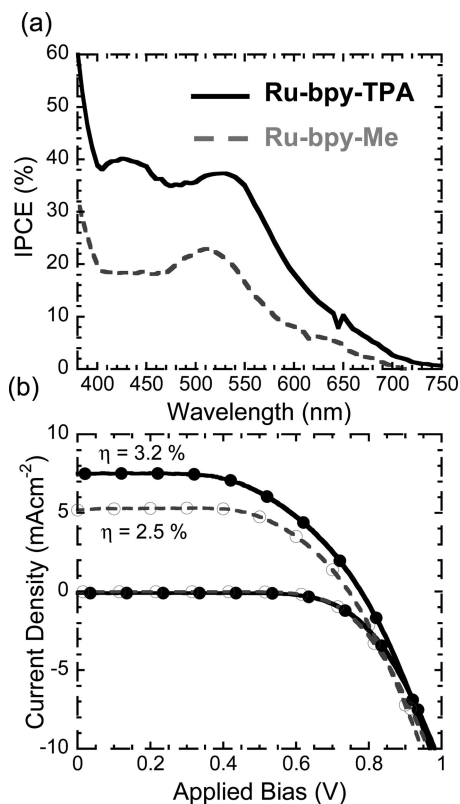


**Figure 3.** (a) Photovoltaic action spectra for complete solid-state dye sensitized solar cells incorporating Ru-bpy-TPA (solid dark curve) and Ru-bpy-Me (dashed gray curve). (b) Current-voltage characteristics measured in the dark and under simulated air mass (AM) 1.5 solar illumination at an intensity of  $100 \text{ mWcm}^{-2}$ .

1-transmission) for the Ru-bpy-TPA device, we would expect a relative drop in IPCE of approximately 15% comparing the peak at 410 nm to that at 540 nm. In our measurements, we do not observe this, with the IPCEs being similar at these two wavelengths. However, in the device configuration, we employ gold electrodes which have a reflectivity of approximately 0.3 at 410 nm and 0.8 and 540 nm.<sup>11</sup> Therefore, accounting for the reflected light but neglecting interference effects and light reflected off the FTO glass, the total fraction of light absorbed in the film is approximately 0.97 at 410 nm and 0.94 at 540 nm, which is comparable, consistent with the IPCE measurements. It is also apparent however that all absorbed photons are not converted to electrons. Considering an approximate 0.1 to 0.2 loss of the incident light due to reflection off, and absorption in, the FTO glass, the internal quantum efficiency at 410 nm is approximately 0.46–0.51. Clearly, even for this well performing dye, there exist significant losses in the photovoltaic process and much room for further improvement.

Figure 3b shows the current-voltage curves measured under simulated air mass (AM) 1.5 solar illumination at an intensity of  $100 \text{ mWcm}^{-2}$  and in the dark. We observe significantly enhanced short-circuit current density and a reasonable increase in the open-circuit voltage ( $\sim 50 \text{ mV}$ ) for the dye with the pendent TPA unit. This results in a significant enhancement in power conversion efficiency from 2.4% to 3.2%. This denotes also a 100% improvement of device performance compared to earlier reports.<sup>6,7</sup>

**Transient Open-Circuit Voltage Decay Measurements.** As can be seen from the increase in the photovoltaic action spectra, the enhanced light absorption has resulted in a significant increase in the charge generation rate. For the cells studied here, the open-circuit voltage should increase by approximately 100

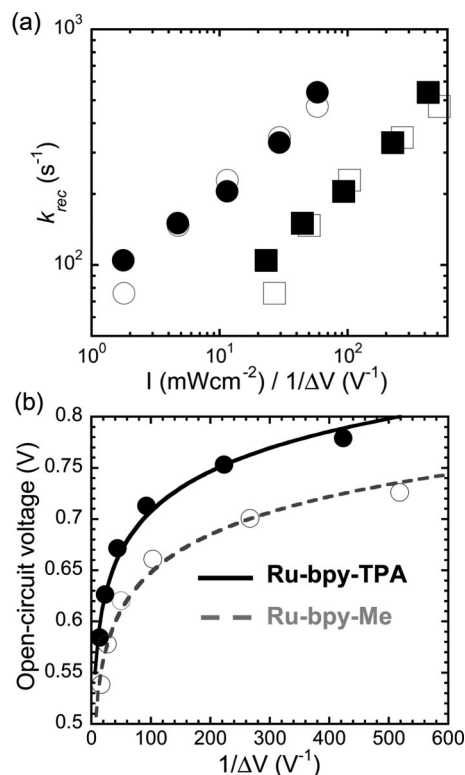


**Figure 4.** (a) Recombination rate constant ( $k_{\text{rec}}$ ), estimated in complete solar cells via a small perturbation open-circuit voltage decay technique, versus white light bias illumination intensity (circles) and versus the reciprocal of the voltage perturbation ( $1/\Delta V$ ) (squares). (b) Open-circuit voltage versus the reciprocal of the voltage perturbation for devices fabricated with the two dyes. This plot reflects the shape of the density-of-states and the relative position in energy of the  $\text{TiO}_2$  states with respect to the reference potential (here the quasi-Fermi level for holes in the Spiro-MeOTAD).

mV per decade increase in the charge generation rate.<sup>8</sup> Here we observe approximately a doubling in the light absorption which should result in a maximum increase in open-circuit voltage of 30 mV. The further enhancement in the open-circuit voltage may be consistent with suppressed electron-hole recombination or a shift in the surface potential at the  $\text{TiO}_2$ /dye/Spiro-MeOTAD interface. In order to investigate this, we have performed transient open-circuit voltage decay measurements to derive the charge recombination lifetime for the two cells: A low intensity square wave pulsed monochromatic light source is superimposed upon a large “bias” white light, with the transient voltage perturbation recorded on a fast source and measuring unit. The decay rate of the voltage perturbation gives a good estimate of the electron recombination rate constant in the cell under conditions similar to solar cell operation.<sup>16</sup> Figure 4a shows the estimated recombination rate constant as a function of bias white light intensity. We find very similar behavior for the cells containing either Ru-bpy-TPA or Ru-bpy-Me, demonstrating that the charge recombination kinetics are weakly influenced by the presence of the TPA units. However, to fully verify this, we need to be certain that the charge density within the film increases in the same manner with light intensity for the two systems.<sup>17</sup> When the small light perturbation pulse is applied to the system (as in the transient open-circuit voltage measurements) new states are filled just above the quasi Fermi level for electrons ( $E_{\text{Fn}}$ ) in the  $\text{TiO}_2$  and the resulting voltage perturbation is proportional to the reciprocal of the density-of-states at  $E_{\text{Fn}}$ . Therefore by plotting the recombination rate constant against the reciprocal of the voltage perturbation ( $1/$

$\Delta V$ ), we compare the recombination rate constant at constant quasi Fermi level position in the  $\text{TiO}_2$  (assuming the same density-of-states in the  $\text{TiO}_2$  for the two systems). This is also shown in Figure 4a. Once again the points lie on similar curves demonstrating little change to the recombination between electrons in the  $\text{TiO}_2$  with holes in the Spiro-MeOTAD for the dyes with or without the TPA units.

From the voltage perturbation measurements we can probe the density of states in the  $\text{TiO}_2$ . As discussed above, the reciprocal of the voltage perturbation ( $1/\Delta V$ ) should scale with the density-of-states at the  $E_{\text{Fn}}$  in the  $\text{TiO}_2$ . We can also consider the open-circuit voltage to be the “splitting” of the quasi Fermi levels, i.e., the difference in energy between the quasi Fermi level for electrons in  $\text{TiO}_2$  and the quasi Fermi level for holes in Spiro-MeOTAD. Therefore, plotting the open-circuit voltage versus  $1/\Delta V$  gives information concerning the shape of the density-of-states and the position of the energy levels in the  $\text{TiO}_2$  with respect to the reference voltage (the reference voltage being the quasi Fermi levels for holes in the Spiro-MeOTAD). This is plotted for the two systems in Figure 4b. Both sets of data fit with very similar logarithmic curves consistent with an exponential tail to the trap density-of-states beneath the conduction band in  $\text{TiO}_2$ . Notably, the curve for the device containing the TPA substituted dye is at a higher position with respect to the reference potential. Since the only alteration between the two systems is the dye, this is consistent with an increased “dipole offset” induced by the Ru-bpy-TPA complex at the  $\text{TiO}_2$ /Dye/Spiro-MeOTAD interface. Since the Ru-bpy-TPA is expected to have some HOMO density located on the TPA unit, this is consistent with the dipole moment for this molecule being larger than that of the Ru-bpy-Me molecule.

## Conclusions

In summary, we have presented a new ruthenium complex with an extended  $\pi$  system and fully characterized it optically, when adsorbed to  $\text{TiO}_2$ , and electronically, when incorporated in solid-state dye-sensitized solar cells. We observe very similar excited-state absorption spectra and recombination kinetics between the electrons in the  $\text{TiO}_2$  with the holes on the dye, when compared to an analog dye without the extended  $\pi$  system. By conjugating the TPA unit to the dye backbone the molecular extinction coefficient has been phenomenally enhanced resulting in far greater light harvesting and photocurrent generation. Positioning the TPA unit away from the  $\text{TiO}_2$  surface appears to have induced a favorable dipole shift, generating an enhanced open-circuit voltage. This contributes significantly to improved solar cell efficiency. Though our results are very encouraging, our estimated internal quantum efficiency (collected electrons

to absorbed photons) for these dyes is only 50%. Hence, by further modification of this type of sensitizer, for example by adding moieties such as oxyethylene chains which have shown significantly enhanced quantum efficiency for standard ruthenium complexes incorporated in solid-state DSCs,<sup>11,18,19</sup> we expect further performance enhancements.

**Acknowledgment.** This work was part funded by EPSRC. A.P. acknowledges Clare College Cambridge and “Fondazione Angelo della Riccia” for funding.

**Supporting Information Available:** Solution UV–vis absorption spectra. This material is available free of charge via the Internet at <http://pubs.acs.org>.

## References and Notes

- (1) Bonhote, P.; Moser, J. E.; Humphry-Baker, R.; Vlachopoulos, N.; Zakeeruddin, S. M.; Walder, L.; Gratzel, M. *J. Am. Chem. Soc.* **1999**, *121* (6), 1324–1336.
- (2) Haque, S. A.; Handa, S.; Peter, K.; Palomares, E.; Thelakkat, M.; Durrant, J. R. *Angew. Chem., Int. Ed.* **2005**, *44* (35), 5740–5744.
- (3) Hirata, N.; Lagref, J. J.; Palomares, E. J.; Durrant, J. R.; Nazeeruddin, M. K.; Gratzel, M.; Di Censo, D. *Chem. Eur. J.* **2004**, *10* (3), 595–602.
- (4) Bach, U.; Lupo, D.; Comte, P.; Moser, J. E.; Weissortel, F.; Salbeck, J.; Spreitzer, H.; Gratzel, M. *Nature* **1998**, *395* (6702), 583–585.
- (5) Nazeeruddin, M. K.; Kay, A.; Rodicio, I.; Humphrybaker, R.; Muller, E.; Liska, P.; Vlachopoulos, N.; Gratzel, M. *J. Am. Chem. Soc.* **1993**, *115* (14), 6382–6390.
- (6) Handa, S.; Wietasch, H.; Thelakkat, M.; Durrant, J. R.; Haque, S. A. *Chem. Commun.* **2007**, (17), 1725–1727.
- (7) Karthikeyan, C. S.; Peter, K.; Wietasch, H.; Thelakkat, M. *Solar Energy Mater. Solar Cells* **2007**, *91*, 432–439.
- (8) Snaith, H. J.; Schmidt-Mende, L.; Chiesa, M.; Gratzel, M. *Phys. Rev. B* **2006**, *74* (1), 045306.
- (9) Ford, T. A.; Avilov, I.; Beljonne, D.; Greenham, N. C. *Phys. Rev. B* **2005**, *71* (12), 119901.
- (10) Pelet, S.; Moser, J. E.; Gratzel, M. *J. Phys. Chem. B* **2000**, *104* (8), 1791–1795.
- (11) Snaith, H. J.; Moule, A. J.; Klein, C.; Meerholz, K.; Friend, R. H.; Graetzel, M. *Nano Lett.* **2007**, *7* (11), 3372–3376.
- (12) Bach, U.; Tachibana, Y.; Moser, J. E.; Haque, S. A.; Durrant, J. R.; Gratzel, M.; Klug, D. R. *J. Am. Chem. Soc.* **1999**, *121* (32), 7445–7446.
- (13) Westerling, M.; Vijila, C.; Osterbacka, R.; Stubb, H. *Phys. Rev. B* **2003**, *67*, 195201.
- (14) Kuang, D.; Klein, C.; Snaith, H. J.; Humphry-Baker, R.; Moser, J.-E.; Zakeeruddin, S. M.; Grätzel, M. *Nano Lett.* **2006**, *6* (4), 769–773.
- (15) Schmidt-Mende, L.; Zakeeruddin, S. M.; Gratzel, M. *Appl. Phys. Lett.* **2005**, *86* (1), 013504.
- (16) O'Regan, B. C.; Lenzmann, F. *J. Phys. Chem. B* **2004**, *108* (14), 4342–4350.
- (17) O'Regan, B. C.; Durrant, J. R. *J. Phys. Chem. B* **2006**, *110* (17), 8544–8547.
- (18) Schmidt-Mende, L.; Kroeze, J. E.; Durrant, J. R.; Nazeeruddin, M. K.; Gratzel, M. *Nano Lett.* **2005**, *5* (7), 1315–1320.
- (19) Snaith, H. J.; Zakeeruddin, S. M.; Schmidt-Mende, L.; Klein, C.; Gratzel, M. *Angew. Chem., Int. Ed.* **2005**, *44* (39), 6413–6417.

JP801714U